JOURNAL OF COMPUTATIONAL PHYSICS 117, 47–54 (1995)

Special Meshes for Finite Difference Approximations to an Advection–Diffusion Equation with Parabolic Layers

ALAN F. HEGARTY

Department of Mathematics and Statistics, University of Limerick, Limerick, Ireland

JOHN J. H. MILLER

Department of Mathematics, Trinity College, Dublin 2, Ireland

EUGENE O'RIORDAN

Department of Mathematics, Regional Technical College, Tallaght, Dublin 24, Ireland

AND

G. I. SHISHKIN

Institute of Mathematics and Mechanics, Russian Academy of Sciences, Ekaterinburg, Russia

Received December 11, 1991; revised July 19, 1993

In this paper a model problem for fluid flow at high Reynolds number is examined. Parabolic boundary layers are present because part of the boundary of the domain is a characteristic of the reduced differential equation. For such problems it is shown, by numerical example, that upwind finite difference schemes on uniform meshes are not ε-uniformly convergent in the discrete L^∞ norm, where ε is the singular perturbation parameter. A discrete L^∞ ε-uniformly convergent method is constructed for a singularly perturbed elliptic equation, whose solution contains parabolic boundary layers for small values of the singular perturbation parameter ε. This method makes use of a special piecewise uniform mesh. Numerical results are given that validate the theoretical results, obtained earlier by the last author, for such special mesh methods.

1. INTRODUCTION

The performance of standard numerical methods for solving singularly perturbed problems depends on the size of the singular perturbation parameter. The typical behavior observed is that the maximum pointwise error *increases* as the mesh is refined until the mesh size is comparable to the width of the relevant boundary layer. This counterintuitive behaviour is not generally known to numerical analysts and engineers who have not worked with singularly perturbed problems. Of course, once the mesh size is comparable to the boundary layer width, the numerical method behaves in the expected classical manner. In practice, singular perturbation problems occur in which the singular perturbation parameter has a wide range of values. One way to obtain solutions with guaranteed accuracy in such cases is to design numerical methods, whose computational performance is independent of the singular perturbation parameter.

Singularly perturbed problems arise, for example, in fluid flow at high Reynolds number, advection-dominated heat and mass transfer, semiconductor device models, and the theory of plates and shells. In this paper, the following linearized form of the Navier–Stokes flow equations is examined,

$$Lu \equiv \varepsilon \Delta u + \mathbf{a} \cdot \Delta u + a_0 u = f \quad \text{in } \Omega = (0, 1) \times (0, 1) \tag{1.1a}$$

$$u = g \quad \text{on } \partial\Omega \tag{1.1b}$$

$$\mathbf{a} = (a_1, a_2), \quad a_1 \geq \alpha_1, \quad a_2 \geq \alpha_2, \quad \alpha_1 + \alpha_2 > 0, \tag{1.1c}$$

where α_1 and α_2 are constants, $a_0(x) \geq 0$ for all $x \in \overline{\Omega}$ and $0 < \varepsilon \leq 1$. The presence of the small parameter ε multiplying the highest derivatives is a characteristic feature of singularly perturbed problems. Small values of ε correspond to large values of characteristic numbers such as the Reynolds number, the Péclet number, or the Hartmann number, which are used in various branches of hydrodynamics and magnetohydrodynamics. Letting $\partial\Omega$ denote the boundary of Ω and letting $\mathbf{n}$ be the outward unit normal, $\partial\Omega$ can be divided into the distinct parts

$$\partial\Omega_V \equiv \{(0, 0), (0, 1), (1, 0), (1, 1)\}$$

$$\partial\Omega_I \equiv \{x \in \partial\Omega \backslash \partial\Omega_V : \mathbf{a} \cdot \mathbf{n} > 0\}$$

$$\partial\Omega_O \equiv \{x \in \partial\Omega \backslash \partial\Omega_V : \mathbf{a} \cdot \mathbf{n} < 0\}$$

$$\partial\Omega_C \equiv \{x \in \partial\Omega \backslash \partial\Omega_V : \mathbf{a} \cdot \mathbf{n} = 0\}$$

0021-9991/95 $6.00

where $\partial\Omega_I$, $\partial\Omega_O$ are the inflow and outflow boundaries, respectively; $\partial\Omega_C$ is the characteristic part of the boundary which, in practice, is a solid boundary, such as the wall of a channel; and $\partial\Omega_V$ is the set of corner points.

For small values of ε, this elliptic problem becomes increasingly hyperbolic in nature, and as $\varepsilon \to 0$ the solution u of (1.1) tends to the solution of the reduced problem,

$$\mathbf{a} \cdot \Delta u + a_0 u = f \quad \text{on } \Omega \tag{1.2a}$$

$$u = g \quad \text{on } \partial\Omega_I. \tag{1.2b}$$

Also, for small values of ε, regular, parabolic, or corner layers may appear; this means that if u is written as the sum,

$$u = u_1 + u_2,$$

where u_1 is the ε-regular component (*i.e.*, derivatives up to first order are bounded uniformly in ε) and u_2 is the ε-singular component (*i.e.*, derivatives up to first order are not ε-uniformly bounded), then the nature of the layer depends on the behaviour of u_2. If the singular component u_2 is described by an ordinary, parabolic, or elliptic differential equation, then the associated layer is said to be a regular, parabolic, or elliptic boundary layer, respectively. A regular boundary layer occurs in a neighbourhood of $\partial\Omega_O$ and a parabolic boundary layer may occur in a neighborhood of $\partial\Omega_C$. The latter arises, for example, in magnetohydrodynamic flow in a rectangular duct under a uniform magnetic field at high Hartmann number (see Temperley [25]). If $u_2 \not\equiv 0$ in the neighbourhood of a corner $c \in \partial\Omega_V$ and if it is the solution of a parabolic or elliptic partial differential equation, then the corresponding layer is called a parabolic or elliptic corner layer, respectively. For a discussion of the various kinds of boundary and corner layers and their asymptotic behaviour, see Vishik and Lyusternik [26], Il'in [10], Shih and Kellogg [17], and the references cited therein. The behavior of parabolic layers is considerably more complicated than that of regular layers. For example, changes in the boundary data near a regular layer do not change the nature of the singular component, whereas near a parabolic layer u_2 may be changed in an essential way. Furthermore, parabolic boundary layers do not arise in one-dimensional problems.

Numerical methods whose solutions converge independently of ε are said to be ε-uniformly convergent. More precisely, a numerical method for solving (1.1) is ε-uniformly convergent of order p on the mesh $\Omega_h = \{(x_i, y_j)\colon i, j = 0, 1, \ldots, N\}$ if

$$\max_{\Omega_h} \|u - u^N\| \leq CN^{-p}, \tag{1.3}$$

where u is the solution of (1.1), u^N is the numerical approximation to u, and the norm is the discrete L^∞ norm on Ω_h. Here, and throughout this paper, C and p denote generic positive constants independent of ε and N (the number of mesh elements).

There are two known classes of ε-uniformly convergent finite difference methods: "fitted operator" methods where, given the mesh, an appropriate finite difference operator is constructed and "special mesh" methods where, given the finite difference operator, an appropriate mesh is constructed. For singularly perturbed ordinary differential equations, fitted operator methods have been constructed and analysed in, for example, Il'in [9], Doolan, Miller, and Schilders [3], O'Riordan and Stynes [14], and Gartland [7]; and special mesh methods have been constructed and analyzed in, for example, Bakhvalov [2], Liseikin and Yanenko [11], and Vulanovich [27]. Both techniques require detailed information about the ε-singular component. The first numerical computations on special meshes of the type analysed by Shishkin were reported in Miller *et al.* [13]. A recent collection of computational methods for the numerical solution of singularly perturbed partial differential equations is contained in Miller [12].

For small values of ε, it is well known that classical numerical methods for (1.1) may produce spurious oscillations throughout the whole domain. Various stable upwind methods have been proposed to control these oscillations. Fitted operator methods for (1.1) have been discussed in, for example, Emel'janov [4–6], Shishkin [18–24], and O'Riordan and Stynes [15] and have been shown to be ε-uniformly convergent in cases where no parabolic layers are present or, more generally, in subdomains not containing the parabolic layers. These methods are fairly obvious extensions to two dimensions of the original fitted operator method proposed by Allen and Southwell [1] and analysed by Il'in [9].

The situation is quite different if the solution of the singularly perturbed problem has a parabolic layer. In [21] Shishkin discusses the singularly perturbed heat equation in the domain $(x, t) \in [0, 1] \times [0, \infty)$. There it is shown that no implicit finite difference method, based on a four-point stencil, on a uniform mesh is ε-uniform for this problem. It is also indicated that a similar result holds for finite difference methods based on more complicated stencils. An outline of the proof is given in [12, pp. 140–141] and numerical computations that support the result experimentally are contained in [16]. A new approach in Shishkin [24] using piecewise-uniform meshes and standard finite difference operators yields methods which are shown theoretically to be ε-uniformly convergent throughout the domain, including the parabolic layers. The main puprose of the present paper is to validate computationally this theoretical result.

In Section 2 a special mesh method which is ε-uniform for all types of layers is described. This method was first introduced by Shishkin in [19]; it uses standard upwind finite difference operators on a special piecewise-uniform mesh, the construction of which is remarkably simple. Numerical results for this method in the case of singularly perturbed problems in two dimensions containing only regular layers are presented in [8].

TABLE I

Maximum Values of $E_{\varepsilon,N}$ for the Upwind Scheme (2.1) on Special Meshes Ω_h^S

ε	$N = 8$	$N = 16$	$N = 32$	$N = 64$	$N = 128$
1.0000000000	.414D − 02	.130D − 02	.526D − 03	.260D − 03	.927D − 04
0.2500000000	.403D − 01	.206D − 01	.982D − 02	.428D − 02	.144D − 02
0.0625000000	.133D + 00	.738D − 01	.398D − 01	.196D − 01	.725D − 02
0.0156250000	.166D + 00	.914D − 01	.494D − 01	.244D − 01	.916D − 02
0.0039062500	.171D + 00	.105D + 00	.559D − 01	.277D − 01	.103D − 01
0.0009765625	.174D + 00	.106D + 00	.577D − 01	.287D − 01	.109D − 01
0.0002441406	.175D + 00	.105D + 00	.585D − 01	.292D − 01	.111D − 01
0.0000610352	.175D + 00	.104D + 00	.589D − 01	.295D − 01	.112D − 01
0.0000152588	.176D + 00	.104D + 00	.591D − 01	.297D − 01	.113D − 01
0.0000038147	.176D + 00	.104D + 00	.592D − 01	.297D − 01	.113D − 01
0.0000009537	.176D + 00	.103D + 00	.592D − 01	.298D − 01	.113D − 01
0.0000002384	.176D + 00	.103D + 00	.592D − 01	.298D − 01	.113D − 01
$\max_\varepsilon E_{\varepsilon,N}$:	.176D + 00	.106D + 00	.592D − 01	.298D − 01	.113D − 01

In Section 3, numerical results are presented for a specific singularly perturbed problem whose solution contains not only regular but also, more importantly, parabolic layers. In Section 4 the numerical results are displayed graphically and features of the visualization are discussed. All calculations are in double-precision Fortran 77 on a DECStation 5000/100. They support the theoretical results obtained by the last author (see [21]).

As was remarked above the numerical methods described in this paper are applied to a simple form of the Navier–Stokes equations. This is linear, two-dimensional, and stationary, and the solution is obtained on a square domain. It should be observed that the constructions and techniques apply to general linear problems on general domains with smooth boundaries. This has been shown theoretically in a long series of papers by the fourth author and computationally in an on-going series of papers by the present authors. The current paper is the first publication known to the authors, which shows experimentally that there are ε-uniform numerical methods for problems with *parabolic* boundary layers. It is conjectured that these constructions and techniques will also lead to good numerical methods for the full Navier–Stokes equations.

It should be noted that here we are not interested in the question of obtaining an optimal mesh. What we want is an ε-uniform method and such methods for problems with parabolic boundary layers have been given only by the fourth author. It is surprising, and not at all obvious, that an ε-uniform method can be obtained by such a simple piecewise uniform mesh. It is evident that for specific problems the mesh can be improved, but great care has to be taken so that the ε-uniform convergence of the method is not lost.

TABLE II

Values of $p_{\varepsilon,N}$ for the Upwind Scheme (2.1) on Special Meshes Ω_h^S

ε	$N = 8$	$N = 16$	$N = 32$	$N = 64$
1.0000000000	1.67	1.31	1.02	1.49
0.2500000000	0.97	1.07	1.20	1.57
0.0625000000	0.85	0.89	1.02	1.43
0.0156250000	0.86	0.89	1.01	1.42
0.0039062500	0.71	0.90	1.01	1.42
0.0009765625	0.71	0.88	1.01	1.40
0.0002441406	0.74	0.84	1.00	1.39
0.0000610352	0.75	0.82	1.00	1.39
0.0000152588	0.76	0.81	0.99	1.39
0.0000038147	0.76	0.81	0.99	1.39
0.0000009537	0.76	0.81	0.99	1.39
0.0000002384	0.76	0.81	0.99	1.39

2. SPECIAL MESHES

The special mesh method, introduced in Shishkin [24], uses standard upwind finite difference operators (denoted by L^U) on a special piecewise-uniform mesh (denoted by Ω_h^S). The special mesh Ω_h^S is chosen so that the finite difference scheme $\{L^U, \Omega_h^S\}$ is ε-uniform. In this section the construction of a special mesh for the general problem (1.1) is described.

For problem (1.1), the upwind finite difference equation

$$L^U u^N \equiv \varepsilon\,(\delta_{\hat{x}_i\hat{x}_i} + \delta_{\hat{y}_j\hat{y}_j})u^N + a_1(x_i, y_j)\delta_{x_i}u^N + a_2(x_i, y_j)\delta_{y_j}u^N + a_0(x_i, y_j)u^N = f(x_i, y_j), \tag{2.1}$$

where

$$\delta_{x_i}u^N \equiv (u^N(x_{i+1}, y_j) - u^N(x_i, y_j))/h_{i+1},$$

$$\delta_{\bar{x}_i}u^N \equiv (u^N(x_i, y_j) - u^N(x_{i-1}, y_j))/h_i,$$

$$\delta_{\hat{x}_i\hat{x}_i}u^N \equiv (\delta_{x_i}u^N - \delta_{\bar{x}_i}u^N)/\bar{h}_i,$$

$$\bar{h}_i \equiv (h_{i+1} + h_i)/2,$$

TABLE III

Maximum Values of $E_{\varepsilon,N}$ for the Upwind Scheme (2.1) on Uniform Meshes Ω_h^U

ε	$N = 8$	$N = 16$	$N = 32$	$N = 64$	$N = 128$
1.0000000000	.414D − 02	.130D − 02	.526D − 03	.260D − 03	.927D − 04
0.2500000000	.403D − 01	.206D − 01	.982D − 02	.428D − 02	.144D − 02
0.0625000000	.188D + 00	.144D + 00	.795D − 01	.402D − 01	.167D − 01
0.0156250000	.120D + 00	.171D + 00	.198D + 00	.166D + 00	.924D − 01
0.0039062500	.927D − 01	.761D − 01	.109D + 00	.174D + 00	.198D + 00
0.0009765625	.405D − 01	.765D − 01	.485D − 01	.606D − 01	.105D + 00
0.0002441406	.105D − 01	.391D − 01	.673D − 01	.444D − 01	.317D − 01
0.0000610352	.265D − 02	.102D − 01	.382D − 01	.625D − 01	.434D − 01
0.0000152588	.665D − 03	.257D − 02	.100D − 01	.377D − 01	.607D − 01
0.0000038147	.166D − 03	.644D − 03	.252D − 02	.989D − 02	.375D − 01
0.0000009537	.416D − 04	.161D − 03	.631D − 03	.294D − 02	.983D − 02
0.0000002384	.104D − 04	.403D − 04	.158D − 03	.624D − 03	.248D − 02
$\max_\varepsilon E_{\varepsilon,N}$:	.188D + 00	.171D + 00	.198D + 00	.174D + 00	.198D + 00

is defined on a general mesh Ω_h. For stability reasons, L^U is used rather than a central finite difference operator to approximate the first-order terms. The construction of a special mesh Ω_h^S depends on the nature and location of the layers. Here the simplest special mesh for problem (1.1) is desribed.

For a regular boundary layer near the outflow boundary $\{x = 0\}$, consider any point $P = (0, y_0)$ on the outflow boundary and partition the line $[0, 1] \times \{y_0\}$ into the two segments $[0, \sigma_x]$ and $[\sigma_x, 1]$, where

$$\sigma_x \equiv \min\left\{\frac{1}{2}, C_1 \varepsilon \ln N\right\}, \quad C_1 > 1/\alpha_1.$$

Both of these segments are partitioned into $N/2$ uniform elements by mesh lines parallel to the outflow boundary. The result is a piecewise uniform rectangular mesh condensing near the boundary $\{x = 0\}$.

Furthermore, if any boundary is a characteristic of the re-

TABLE IV

Maximum Values of $E_{\varepsilon,N}$ for the Upwind Scheme (2.1) on Naïve Meshes $\tilde{\Omega}_h$

ε	$N = 8$	$N = 16$	$N = 32$	$N = 64$	$N = 128$
1.0000000000	.414D − 02	.130D − 02	.526D − 03	.260D − 03	.927D − 04
0.2500000000	.425D − 01	.214D − 01	.102D − 01	.457D − 02	.173D − 02
0.0625000000	.150D + 00	.102D + 00	.685D − 01	.400D − 01	.185D − 01
0.0156250000	.196D + 00	.157D + 00	.125D + 00	.944D − 01	.739D − 01
0.0039062500	.204D + 00	.177D + 00	.158D + 00	.140D + 00	.118D + 00
0.0009765625	.206D + 00	.183D + 00	.170D + 00	.159D + 00	.148D + 00
0.0002441406	.207D + 00	.219D + 00	.172D + 00	.166D + 00	.159D + 00
0.0000610352	.224D + 00	.263D + 00	.244D + 00	.181D + 00	.164D + 00
0.0000152588	.236D + 00	.287D + 00	.289D + 00	.255D + 00	.185D + 00
0.0000038147	.242D + 00	.300D + 00	.314D + 00	.301D + 00	.260D + 00
0.0000009537	.245D + 00	.306D + 00	.327D + 00	.327D + 00	.307D + 00
0.0000002384	.247D + 00	.309D + 00	.334D + 00	.340D + 00	.333D + 00
0.0000000596	.247D + 00	.311D + 00	.338D + 00	.347D + 00	.347D + 00
0.0000000149	.248D + 00	.312D + 00	.339D + 00	.351D + 00	.354D + 00
0.0000000037	.248D + 00	.312D + 00	.340D + 00	.353D + 00	.357D + 00
0.0000000009	.248D + 00	.312D + 00	.341D + 00	.353D + 00	.359D + 00
0.0000000002	.248D + 00	.312D + 00	.341D + 00	.354D + 00	.360D + 00
0.0000000001	.248D + 00	.312D + 00	.341D + 00	.354D + 00	.360D + 00
$\max_\varepsilon E_{\varepsilon,N}$:	.248D + 00	.312D + 00	.341D + 00	.354D + 00	.360D + 00

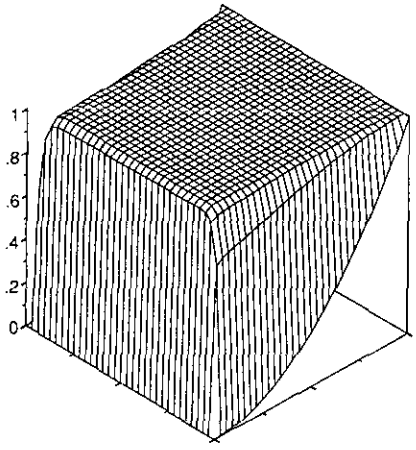

FIG. 4.1. *Surface plot of numerical solution on uniform mesh* Ω_h^U: $\varepsilon = 0.0009765625$; $N = 32$.

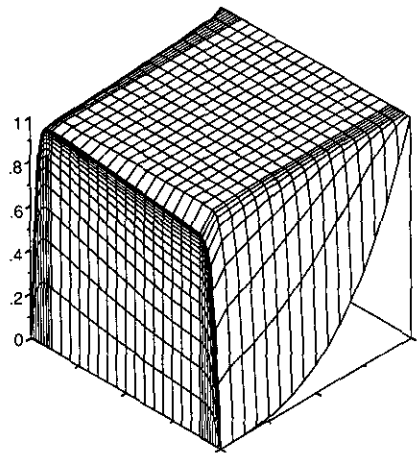

FIG. 4.3. Surface plot of numerical solution on uniform mesh Ω_h^S: $\varepsilon = 0.0009765625$; $N = 32$.

duced problem, a parabolic boundary layer occurs in its neighborhood and the following construction is required. For example, if $\{y = 0\}$ is characteristic, consider any point $Q = (x_0, 0)$ on this boundary and partition the line $\{x_0\} \times [0, \frac{1}{2}]$ into the two segments $[0, \sigma_y]$ and $[\sigma_y, \frac{1}{2}]$, where

$$\sigma_y \equiv \min\left\{\frac{1}{4}, \sqrt{\varepsilon} \ln N\right\}.$$

Both of these segments are partitioned into $N/4$ uniform elements by mesh lines parallel to this boundary. If the boundary $\{y = 1\}$ is also characteristic an analogous construction is used. The final result is a piecewise uniform rectangular mesh condensing near the boundaries $\{x = 0\}$, $\{y = 0\}$, $\{y = 1\}$.

These rules define a special mesh throughout the whole domain. If corner layers exist, it is not necessary to adapt the above construction. The special mesh Ω_h^S defined above automatically deals with corner layers, as has been shown by Shishkin [24]. In fact, the finite difference scheme $\{L^U, \Omega_h^S\}$ described above is ε-uniform for all types of layers. More precisely, if $a_1 > 0$, $a_2 > 0$, a_1, a_2, a_0, f, g are sufficiently smooth, and certain compatibility conditions are satisfied so that only regular boundary layers appear, then it is proved in [24] that

$$\|u - u^N\|_\infty \leq CN^{-1} \ln N.$$

On the other hand, if the compatibility conditions are not satisfied and non-regular corner layers appear, then

$$\|u - u^N\|_\infty \leq C(N^{-1} \ln N)^p, \quad p = \tfrac{1}{14}.$$

Moreover, if $a_2 \equiv 0$, then parabolic layers appear and the following estimate holds:

$$\|u - u^N\|_\infty \leq C(N^{-1} \ln N)^p, \quad p = \tfrac{1}{18}.$$

More precise statements of these results may be found in Shishkin [24].

The above theoretical estimates of the order of ε-uniform convergence are true for general n-dimensional singularly perturbed problems. We remark that the numerical estimates given below for the rates of ε-uniform convergence for specific two-dimensional problems are considerably better, which suggests that these theoretical results are not as sharp as possible.

It is important to note that the simpler, but naïve, choice of the points

$$\tilde{\sigma}_x \equiv \left\{\frac{1}{2}, \varepsilon\right\}, \quad \tilde{\sigma}_y \equiv \left\{\frac{1}{4}, \sqrt{\varepsilon}\right\} \tag{2.2}$$

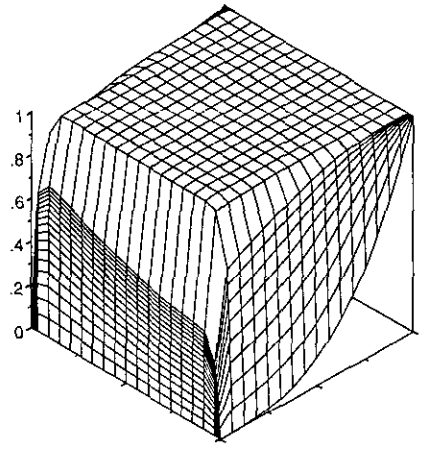

FIG. 4.2. Surface plot of numerical solution on naïve mesh $\tilde{\Omega}_h$: $\varepsilon = 0.0009765625$; $N = 32$.

does *not* yield an ε-uniform numerical method for this problem. This can be shown both theoretically and computationally for this and more general problems.

3. NUMERICAL SOLUTION USING A SPECIAL MESH METHOD

For the specific problem

$$\varepsilon\Delta u + (1 + x^2 + y^2)u_x = 0 \quad \text{on } \Omega = (0, 1) \times (0, 1) \tag{3.1a}$$

$$u(x, 0) = x^3, \quad u(x, 1) = x^2, \quad u(0, y) = 0, \quad u(1, y) = 1, \tag{3.1b}$$

numerical results are given for the upwind finite difference equation

$$\varepsilon(\delta_{x_i x_i} u^N + \delta_{y_j y_j} u^N) + (1 + x_i^2 + y_j^2)\delta_{x_i} u^N = 0 \tag{3.2a}$$

$$u^N = u \quad \text{on } \partial\Omega_h \tag{3.2b}$$

on special meshes $\Omega_h^S \equiv \{(x_i^S, y_j^S)\}$, where

$$x_i^S = \begin{cases} 2i\sigma_x/N & \text{for } i = 0, 1, \ldots, N/2, \\ \sigma_x + 2(i - N/2)(1 - \sigma_x)/N & \text{for } i = N/2, \ldots, N; \end{cases}$$

$$y_j^S = \begin{cases} 4j\sigma_y/N & \text{for } j = 0, 1, \ldots, N/4, \\ \sigma_y + 2(j - N/4)(1 - 2\sigma_y)/N & \text{for } j = N/4, \ldots, 3N/4, \\ (1 - \sigma_y) + 4(j - 3N/4)(\sigma_y)/N & \text{for } j = 3N/4, \ldots, N; \end{cases}$$

and

$$\sigma_x \equiv \min\left\{\frac{1}{2}, \varepsilon \ln N\right\}, \quad \sigma_y \equiv \min\left\{\frac{1}{4}, \sqrt{\varepsilon} \ln N\right\}.$$

This problem has a regular layer at the outflow boundary $\{x = 0\}$ and two parabolic layers, one along the bottom wall $\{y = 0\}$ and one along the top wall $\{y = 1\}$. Note that the boundary conditions are only C^0 compatible at the corners.

The construction of these special meshes follows the general guidelines given in Section 2. Numerical results for problem (3.1) using the upwind finite difference operator (2.1) and these special meshes are given in Table I.

The errors $|u^N(x_i, y_j) - u(x_i, y_j)|$ are approximated for successive values of ε and $N = 8, 16, 32, 64, 128$ by $e_{\varepsilon,N}(i, j) = |u^N(x_i, y_j) - u_{\text{comp}}(x_i, y_j)|$, where u_{comp} is the best computed approximation to the exact solution u, which is defined at each point of Ω by bilinear interpolation of the finite difference solution on the finest available mesh ($N = 256$). For each ε the maximum absolute error is approximated by

$$E_{\varepsilon,N} = \max_{1 \le i,j \le N-1} e_{\varepsilon,N}(i, j).$$

In Table I $E_{\varepsilon,N}$ decreases for each ε as N increases; it follows that convergence rates for each ε and for $N = 8, 16, 32, 128$ can be estimated by $p_{\varepsilon,N}$, where

$$p_{\varepsilon,N} = \log_2\left(\frac{E_{\varepsilon,N}}{E_{\varepsilon,2N}}\right).$$

These approximate convergence rates are shown in Table II.

Tables I and II numerically confirm the fact that the upwind finite difference operator (2.2) with the special mesh Ω_h^S is ε-uniformly convergent. It is also interesting to note that the order of convergence increases with increasing N in each row of Table I, apart from the first. The entries in the columns of Table I underestimate the maximum absolute errors, especially for $N = 128$, since u_{comp} has been used instead of the (unknown) exact solution; hence, the entries in the last column of Table II overestimate the convergence rates for $N = 64$. Nonetheless, the values of $p_{\varepsilon,N}$ are consistent with an actual ε-uniform convergence rate of approximately 1, in contrast to the theoretical rate of $\frac{1}{18}$ quoted in Section 2. It is important to note that the rapid change in mesh size in the direction normal to the boundary layer does not appear to affect the computational performance of the numerical method adversely. This is seen from the fact that the number of iterations required to solve all of the linear systems encountered in the present work is found to be independent of ε.

Having established that the standard upwind finite difference operator (2.1) with the special mesh Ω_h^S is ε-uniformly convergent, the computed absolute errors for (2.1) using uniform and naïve meshes can now be approximated by $e_{\varepsilon,N}^S(i, j) = |u^N(x_i, y_j) - u_{\text{comp}}(x_i, y_j)|$. Again, for each ε the maximum nodal error is approximated by

$$E_{\varepsilon,N} = \max_{i,j} e_{\varepsilon,N}(i, j),$$

and these maximum computed absolute errors are given in Tables III and IV for uniform meshes and naïve meshes $\tilde{\Omega}_h$—with $\tilde{\sigma}_x$ and $\tilde{\sigma}_y$ as defined in (2.2)—respectively.

The maximum computed absolute errors $E_{\varepsilon,N}$ in the case of naïve meshes $\tilde{\Omega}_h$ are much larger than those in the case of uniform meshes; this occurs because the uniform meshes have no elements in the boundary layers for small values of ε. The latter fact is evident from the graphs presented in the next section.

4. VISUALIZATION OF THE NUMERICAL RESULTS

In this section numerical solutions obtained using the standard upwind finite difference operator (2.1), with each of the three types of mesh discussed above, are plotted. In each of

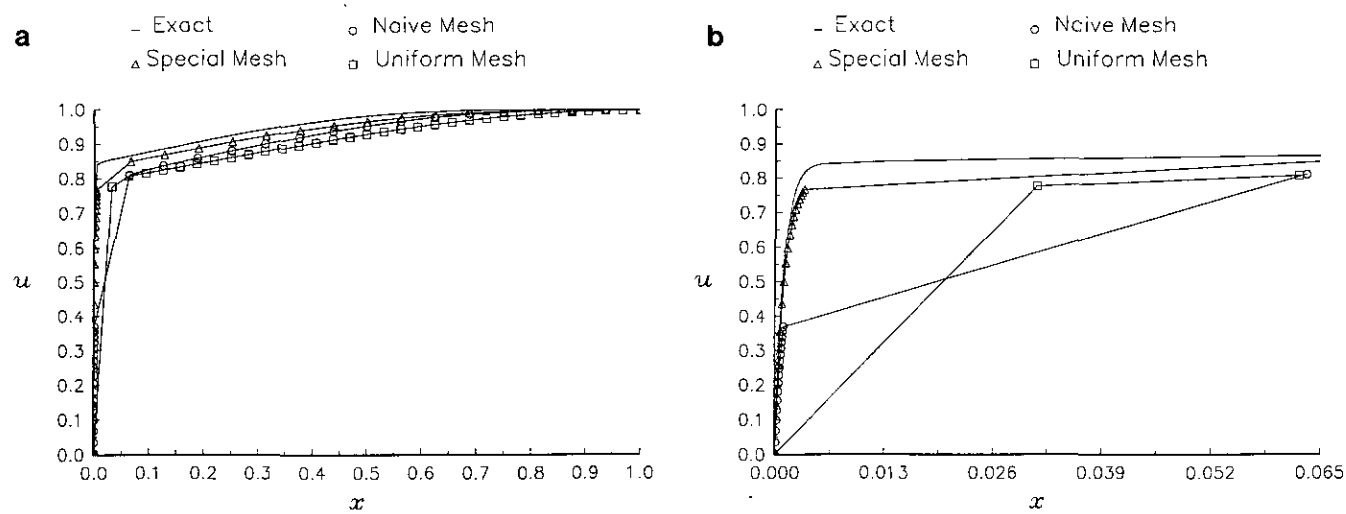

FIG. 4.4. (a) Cross-section of numerical solutions along the line $y = 0.05$; (b) cross-section of numerical solutions along the line $y = 0.05$ between $x = 0$ and $x = 0.065$. $\varepsilon = 0.0009765625$ and $N = 32$.

the figures $\varepsilon = 0.0009765625$ and $N = 32$, because for these values the boundary layers are easily observable.

Figure 4.1 displays a surface plot of the numerical solution of problem (3.1) obtained using the upwind finite difference operator (3.2) with a uniform mesh. The surface plot Fig. 4.1 gives the impression that the boundary layers are resolved by this method but, in fact, there are no mesh elements inside the regular layer and few inside the parabolic layer. As $\varepsilon \to 0$ the number of elements inside the parabolic layer also goes to 0.

Figure 4.2 displays a surface plot of the numerical solution of problem (3.1) obtained using the upwind finite difference operator (3.2) with the naïve mesh $\tilde{\Omega}_h$. It is apparent from Fig. 4.2 that, using the naïve mesh, too many mesh elements are concentrated close to the boundaries Ω_O and Ω_C and not enough are at the outer edges of the boundary layers.

Figure 4.3 displays a surface plot of the numerical solution of problem (3.1) obtained using the upwind finite difference operator (3.2) with the special mesh Ω_h^S. It is easy to see in Figure 4.3 that both the parabolic and regular layers are resolved accurately.

Finally some one-dimensional cross-sections of the numerical solutions shown above are compared with the "exact" solution u_{comp}. Figures 4.4 show cross sections of the numerical solutions at $y = 0.05$ (inside one of the parabolic layers) and Fig. 4.5 shows cross sections of the numerical solutions at $x = 0.005$ (inside the regular layer). None of the meshes has mesh lines at these values; therefore, all of the numerical solutions illustrated are obtained by linear interpolation of the numerical solutions from the adjacent mesh lines. Figure 4.4a may give the impression that the computed solution on $\tilde{\Omega}_h$ is more accurate than that on Ω_h^S, but Fig. 4.4b shows that near the edge of the regular layer the computed solution on Ω_h^S is considerably more accurate; indeed it may be noted that the computed solution on Ω_h^U is more accurate than that on $\tilde{\Omega}_h$ in the neighbourhood of $x = 0.03$. It should also be noted that the constant C_1 which defines σ_x, as defined in Section 2 has been chosen to be 1 here; Fig. 4.4 would seem to indicate that this is not the optimal value. In the case of Fig. 4.5 it is clear that the computed solution on the special mesh most accurately resolves the parabolic layers and is also the most accurate solution outside the layers. Figure 4.5 also demonstrates that it is impossible for a finite difference method on a uniform mesh to approximate the exact solution inside any boundary layer.

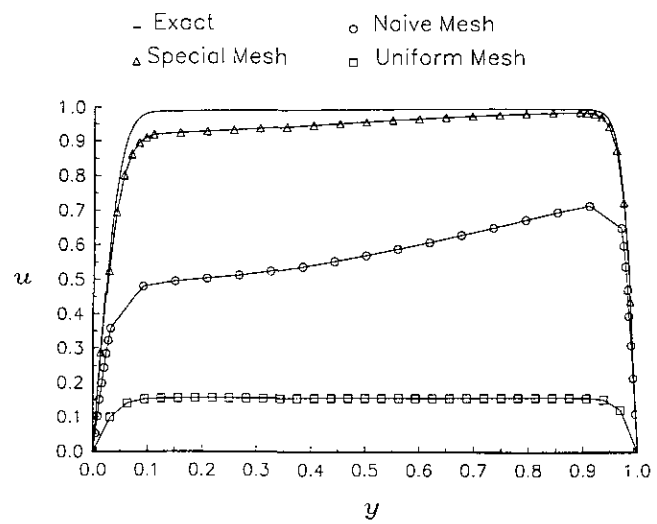

FIG. 4.5. Cross-section of numerical solutions along the line $x = 0.005$: $\varepsilon = 0.0009765625$; $N = 32$.

5. CONCLUSIONS

Upwind finite difference schemes using uniform, naïve, and special meshes were examined. Computations for a specific

problem with parabolic boundary layers were reported. It was shown that ε-uniform convergence is obtained only when a special mesh is used. The ε-uniform rate of convergence achieved in practice is significantly better than the rates predicted by theoretical investigations. The paper contains the first ε-uniform numerical results known to the authors for a problem with parabolic boundary layers.

ACKNOWLEDGMENTS

The authors appreciate the helpful comments and suggestions received from the editor and one of the referees.

REFERENCES

1. D. N. de G. Allen and R. V. Southwell, *Quart. J. Mech. Appl. Math.* **8**(2), 129 (1955).
2. N. S. Bakhvalov, *J. Vychisl. Mat. i Mat. Fis.* **9**(4), 841 (1969).
3. E. P. Doolan, J. J. H. Miller, and W. H. A. Schilders, *Uniform Numerical Methods for Problems with Initial and Boundary Layers* (Boole, Dublin, 1980).
4. K. V. Emel'janov, *Numer. Methods Mech. Cont. Media* **1**(5), (1970).
5. K. V. Emel'janov, in *Boundary Value Problems for Equations of Mathematical Physics* (USSR Academy of Sciences, Ural Scientific Centre, Russia, 1973), p. 30.
6. K. V. Emel'janov, *Difference Methods for the Solution of Boundary Problems with Discontinuous Boundary Data,* edited by G. I. Shishkin (Sverdlovsk, 1976), p. 19.
7. E. C. Gartland, Jr., *Math. Comput.* **48,** (1987).
8. A. F. Hegarty, J. J. H. Miller, E. O'Riordan, and G. I., Shishkin, submitted.
9. A. M. Il'in, *Mat. Zametki* **6**(237), (1969); *Math Notes* **6**(596), (1969).
10. A. M. Il'in, *BAIL IV, Proceedings, Fourth International Conference on Interior and Boundary Layers, 1986,* edited by J. J. H. Miller, p. 98.
11. V. D. Liseikin and N. N. Yanenko, in *BAIL III, Proceedings, Third International Conference on Interior and Boundary Layers, 1984,* edited by J. J. H. Miller, p. 68.
12. J. J. H. Miller (Ed.), *Computational Methods for Boundary and Interior Layers in Several Dimensions* (Boole, Dublin, 1991).
13. J. J. H. Miller, E. Mullarkey, E. O'Riordan, and G. I. Shishkin, *C. R. Acad. Sci. Paris Ser. I.* **312,** 643 (1991).
14. E. O'Riordan and M. Stynes, in *BAIL IV, Proceedings, Fourth International Conference on Interior and Boundary Layers, 1986,* edited by J. J. H. Miller, p. 157.
15. E. O'Riordan and M. Stynes, *Math. Comput* **57**(195), 47 (1991).
16. E. O'Riordan, A. F. Hegarty, and M. Stynes, in *Numerical Methods in Singularly Perturbed Problems.* Technische Universitat, Dresden, March 1991, p. 91.
17. S. D. Shih and R. B. Kellogg, *SIAM J. Math. Anal.* **18,** 1467 (1987).
18. G. I. Shishkin, *USSR Comput. Maths. Math. Phys.* **26,** 38 (1986).
19. G. I. Shishkin, *Sov. J. Numer. Anal. Math. Modelling* **3**(5), 393 (1988).
20. G. I. Shishkin, *J. Vychisl. Mat. i. Mat. Fis.* **28**(11), 1649 (1988).
21. G. I. Shishkin, *USSR Comput. Maths. Math. Phys.* **29**(4), 1 (1989).
22. G. I. Shishkin, in *Proceedings, Conf. Discretization Methods in Singular Perturbations and Flow Problems, Technical University, Magdeburg, DDR, May 1989,* p. 73.
23. G. I. Shishkin, *Sov. J. Numer. Anal. Math Modelling* **4**(1), 69 (1989).
24. G. I. Shishkin, second doctoral thesis, Keldysh Institute of Applied Mathematics, USSR Academy of Sciences, Moscow, 1990.
25. D. J. Temperley and L. Todd, *Proc. Cambridge Philos. Soc.* **68,** 337 (1971).
26. J. K. Vishik and L. A. Lyusternik, *Uspekhi. Mat. Nauk* **12**(5), 3 (1957); *Am. Math. Soc. Transl.* (2) **20,** 239 (1962).
27. R. Vulanovic, *Rev. Res. Faculty Science Univ. Novi-Sad, Ser. Mat.* **13,** 187 (1983).